International Journal of Pharmaceutics xxx (2013) xxx–xxx

Contents lists available at SciVerse ScienceDirect

International Journal of Pharmaceutics

journal homepage: www.elsevier.com/locate/ijpharm

Pharmaceutical nanotechnology

Synergistic targeted delivery of payload into tumor cells by dual-ligand liposomes co-modified with cholesterol anchored transferrin and TAT

Q1 Jie Tang[a,1], Li Zhang[a,1], Yayuan Liu[a], Qianyu Zhang[a], Yao Qin[a], Yujia Yin[a], Wenmin Yuan[a], Yuting Yang[a], Yafei Xie[a], Zhirong Zhang[a], Qin He[a,b,*]

[a] Key Laboratory of Drug Targeting and Drug Delivery Systems, Ministry of Education, West China School of Pharmacy, Sichuan University, Chengdu, Sichuan 610041, People's Republic of China
[b] Key Laboratory of Smart Drug Delivery, Ministry of Education & PLA, Fudan University, Shanghai 201203, People's Republic of China

ARTICLE INFO

Article history:
Received 4 April 2013
Received in revised form 15 May 2013
Accepted 13 June 2013
Available online xxx

Keywords:
Dual-ligand
Synergistic effect
Transferrin
Cell penetrating peptide
Liposomes

ABSTRACT

This study was mainly focused on developing a dual-ligand liposomal delivery system to enhance both targeting specificity and cellular uptake. The specific ligand transferrin (TF) and the cationic cell-penetrating peptide TAT were connected with cholesterol *via* a polyethylene glycol (PEG) spacer to prepare the dual-ligand liposomes (TAT/TF-PEG-LP). Then the *in vitro* cellular uptake by three kinds of cells that possessed different expressing levels of transferrin receptor (TFR) and the *in vivo* delivery efficiency were evaluated. Compared to the single-ligand TAT or TF modified liposomes (TAT-PEG-LP or TF-PEG-LP), TAT/TF-PEG-LP exhibited the enhanced cellular uptake and selectivity *via* the synergistic effect of both ligands *in vitro*. The *ex vivo* fluorescence imaging of tumors, the qualitative observation of tumor frozen section and the quantitative determination of cellular uptake in tumor tissues altogether showed the *in vivo* delivery efficiency of TAT/TF-PEG-LP was higher than that of other liposomes. In conclusion, the dual-ligand liposomes co-modified with TF and TAT possessed a strong capability for synergistic targeted delivery of payload into tumor cells both *in vitro* and *in vivo*.

1. Introduction

Cancer has become a horrible disease because of its dramatic incidence, low recovery rate and high mortality. In the last two decades, liposomal drug delivery systems hold extraordinary potential for delivery of therapeutics to tumor, various strategies have been used to improve their targeting specificity and cellular uptake. PEGylation has been extensively employed to enhance the accumulation of liposomes in tumor tissues through enhanced permeability and retention (EPR) effects, which was the passive form of targeting. In attempts to increase the specificity of interaction between liposomes and tumor cells, recent efforts in the liposome field have been focusing on the development of the active tumor targeted liposomes, which were modified with some specific ligands such as TF, folic acid, peptides or antibodies, and could selectively recognize and bind to the specific receptor over-expressed on tumor cells, resulting in increased targeting efficiency and less toxicity. Among various kinds of active targeting moieties, TF is a very suitable candidate for cancer therapeutics. The overexpression of TFR on many kinds of tumor cells makes this glycoprotein an effective and widely explored target for site-specific delivery of anti-tumor drug to tumors (Singh, 1999; Anabousi et al., 2006). Besides, as an endogenous blood glycoprotein (Suzuki et al., 2007), the incorporation of TF in PEGylated liposomes would not bring a detrimental impact on reticuloendothelial system (RES) evasion *in vivo* compared with some other active targeting moieties (McNeeley et al., 2007; Gabizon et al., 2003).

However, the presence of receptor-targeting moiety alone on PEGylated liposomes limits the cellular uptake of liposomes due to receptor saturation (Kibria et al., 2011; Sharma et al., 2012). Considering that an ideal tumor targeted drug delivery system should not only selectively targeted delivery drugs to tumor, but also deliver the drugs into tumor cells with high efficacy, the receptor saturation needed to be overcame. In previous studies, the cell-penetrating peptides (CPPs) conjugated to the surface of liposomes have been widely investigated under *in vitro* conditions for increasing the intracellular delivery of drugs (Wadia and Dowdy, 2002). And the cationic cell-penetrating peptide CPP (TAT) derived

* Corresponding author at: West China School of Pharmaceutics, Sichuan University, #17 Section 3, Southern Renmin Nan Road, Chengdu Municipality 610041, Sichuan Province, People's Republic of China. Tel.: +86 28 85502532; fax: +86 28 85502532.
E-mail addresses: qinhe@scu.edu.cn, qinhe317@126.com (Q. He).
[1] These authors contributed equally to this work.

0378-5173/$ – see front matter © 2013 Elsevier B.V. All rights reserved.
http://dx.doi.org/10.1016/j.ijpharm.2013.06.048

from the HIV-1 protein TAT could facilitate the intracellular delivery of cargoes with various sizes and physicochemical properties (Banks et al., 2005; Brooks et al., 2005; Gupta et al., 2005). Liposomes modified with TAT could deliver the cargoes into cells with high efficiency *via* an unsaturated and receptor/transporter independent pathway (Torchilin et al., 2001). Here we followed a dual mechanistic approach for targeting TFR on tumor cells and further improving the cellular uptake of the targeted delivery vehicle. We combined the receptor targeting property of TF with the enhanced cell uptake effect of TAT to improve the transport of desired cargoes to tumor.

In this study, cholesterol, an important component in liposomal formulations, was used as a lipid anchor to connect with PEG to form the cholesterol derivative lipids (CHO-PEG). To develop the dual-ligand liposome modified with TAT and TF, the active targeting ligand TF was covalently conjugated with the CHO-PEG_{3500}, and TAT was attached to the distal end of a shorter CHO-PEG_{2000}. As we all known, TAT is a nonspecific functional molecule, which penetrates any cells (Torchilin et al., 2001), besides, the positive charge of TAT would increase the instability and toxicity of liposomes *in vivo*. These drawbacks limit the use of TAT in systemic administration. But here the PEG chain length difference of two functional materials in liposomal formulations could ensure TAT to be shielded during circulation, then overcame the non-specificity, instability and toxicity of liposomes caused by TAT *in vivo*. In this liposomal formulation, TF with a longer PEG chain could help targeting tumor cells, and at the same time mask the non-specificity of TAT, after binding to target cells, TAT could mightily enhance cellular uptake, which resulted in increased targeting specificity and cellular uptake efficiency. To verify the synergistic effect of dual-ligand liposomes on cellular uptake, we assessed its cellular uptake efficiency compared with PEG-LP and single-ligand liposomes (TAT-PEG-LP and TF-PEG-LP) *in vitro*. And to further validate the cell specificity, we compared the differences of synergistic effect between three kinds of cells that possessed different expressing levels of TFR. For the *in vivo* study, we firstly investigated the distribution in tumors *via ex vivo* fluorescence imaging, then the capability for the synergistic targeted delivery of payload into tumor cells was further qualitatively evaluated *via* confocal laser scanning microscopy and quantitatively determined *via* flow cytometer.

2. Materials and methods

2.1. Materials

Soybean phospholipids (SPC) were purchased from Shanghai Taiwei Chemical Company (Shanghai, China), and cholesterol (CHO) was purchased from Chengdu Kelong Chemical Company (Chengdu, China). The PEG functional materials with different chain lengths (NHS-$PEG_{2000/3500}$-MAL and mPEG_{2000}-NHS) were all purchased from JENKEM Technology (Beijing, China). 1,2-Dioleoyl-sn-glycero-3-phosphoethanolamine-N-(carboxyfluorescein) (CFPE) was purchased from Avanti Lipids (USA). TAT peptide with terminal cysteine (Cys-AYGRKKRRQRRR) was synthesized according to the standard solid phase peptide synthesis by Chengdu KaiJie Bio-pharmaceutical Co., Ltd. (Chengdu, China). 1,1′-Dioctadecyl-3,3,3′,3′-tetramethylindodicarbocyanine 4-chlorobenzenesulfonate salt (DiD) was purchased from Biotium (USA). Holo-Transferrin human was purchased from Sigma (USA). Fluorescein isothiocyanate (FITC) labeled anti-CD71 antibodies was purchased from Beckman Coulter Inc. (USA). Collagenase type IV and DNase I were purchased from Biosharp. The other chemicals were obtained from commercial sources.

2.2. Synthesis of CHO-PEG_{2000}-TAT/CHO-PEG_{3500}-TF

2.2.1. Synthesis of compound 5

The compound **5** was synthesized as outlined in Fig. 1. Cholesterol **1** and p-toluenesulfonyl chloride (molar ratio = 1:2) in anhydrous pyridine was stirred for 16 h at room temperature. After purification by a silica-gel chromatography column with $CHCl_3$/EtOAc (9:1) as the eluant, the cholesterol p-toluenesulfonate was obtained. Then product **2** and diglycol (DEG) (molar ratio = 1:8) were dissolved in dry 1,4-dioxane. The reaction mixture was

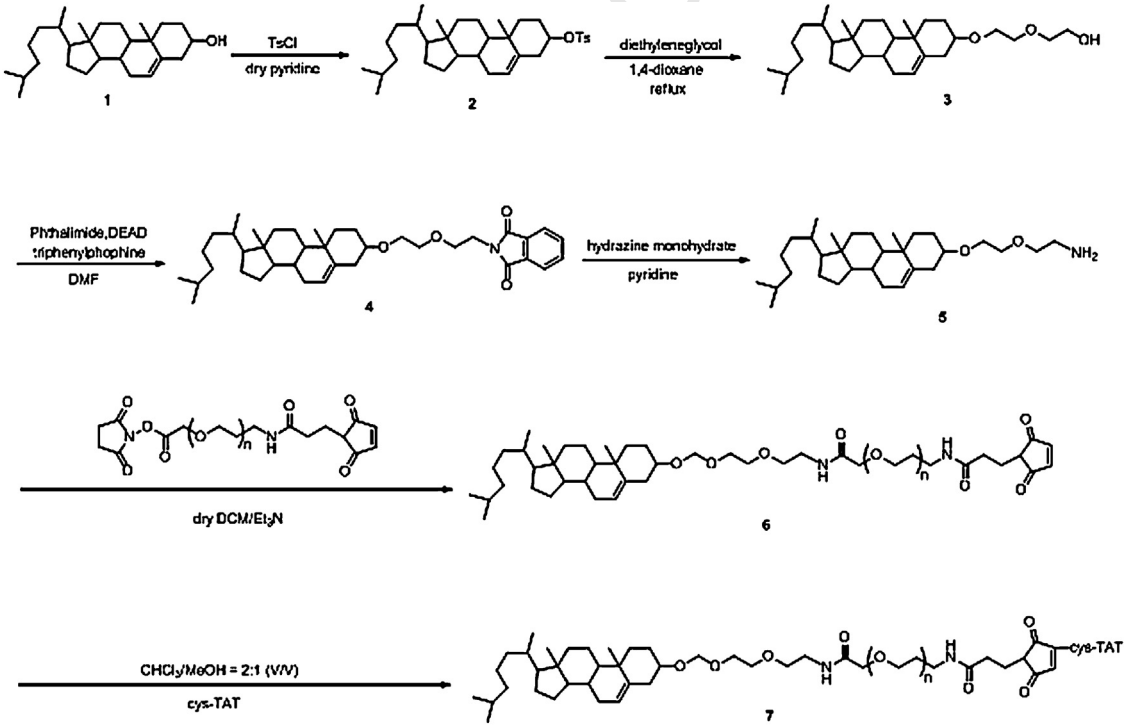

Fig. 1. Schematic of synthesis of the compounds **5** and **7**. The synthesis was confirmed by ^{1}H NMR, mass spectroscopy.

Please cite this article in press as: Tang, J., et al., Synergistic targeted delivery of payload into tumor cells by dual-ligand liposomes co-modified with cholesterol anchored transferrin and TAT. Int J Pharmaceut (2013), http://dx.doi.org/10.1016/j.ijpharm.2013.06.048

refluxed overnight to give the compound **3**. After that, to the solution of **3** (1 equiv.) in dry DMF, phthalimide (5 equiv.), triphenylphosphine (5 equiv.), and diethylazodicarboxylate-toluene (5 equiv.) was added one by one, the mixture was stirred at room temperature for 4 h. The crude product was purified on a silica-gel chromatography column to get **4**. Then the prepared **4** (1 equiv.) in pyridine was added to the solution of hydrazine monohydrate (5 equiv.), and the mixture was stirred at room temperature for 24 h to give the desired compound **5**. The chemical structure was verified by ^{1}H NMR (Shohda and Sugawara, 2006; Pan et al., 2007).

2.2.2. Synthesis of CHO-PEG$_{2000}$-TAT (compound 7)

The compound **5** was reacted with NHS-PEG$_{2000}$-MAL (molar ratio = 2:1) in dry dichloromethane (DCM) at room temperature under argon in the presence of triethylamine for about 4 h. After the thin layer chromatography (TLC) (DCM/MeOH/H_2O = 3:0.5:0.001) showed the disappearance of NHS-PEG$_{2000}$-Mal, the reaction mixture was filtered and the filtrate was evaporated under vacuum. Excess **5** was removed by adding 5 ml of acetonitrile to precipitate it, and the mixture was kept at 4 °C overnight. Then it was centrifuged at 5000 rpm for 10 min. After that, the supernatant was collected and evaporated again under vacuum to get the dry **6** (CHO-PEG$_{2000}$-MAL).

The CHO-PEG$_{2000}$-MAL and Cys-TAT (molar ratio = 1:1.5) were reacted in the mixture of $CHCl_3$/MeOH (V:V = 2:1) with gentle stirring at room temperature for about 30 h (Qin et al., 2011). After TLC (DCM/MeOH/H_2O = 3:0.75:0.12) showed the disappearance of CHO-PEG$_{2000}$-MAL, the mixture was evaporated under vacuum, the slight excess of Cys-TAT was removed by adding a small volume of $CHCl_3$, the insoluble material was filtered, and the supernatant was evaporated again under vacuum to afford compound **7** (Fig. 1).

2.2.3. Synthesis of CHO-PEG$_{3500}$-TF

After the compound **6** (CHO-PEG$_{3500}$-MAL) was well prepared as given in Section 2.2.2, we synthesized CHO-PEG$_{3500}$-TF as described previously (Yang et al., 2008; Hatakeyama et al., 2004; Chiu et al., 2006) with some modification. Briefly, TF in phosphate balanced solution (PBS pH 8) reacted with 5× Traut's reagent to yield TF-SH. Free Traut's reagent was removed by passing the Sephadex G50 column. CHO-PEG$_{3500}$-MAL was made into micelles with a concentration of 1 mg/ml. Then TF-SH was coupled to micelles of CHO-PEG$_{3500}$-MAL at a protein-to-lipid molar ratio of 1:10 for 4 h at 25 °C. Lastly, 10 mg/ml MEA was added to the mixture to end the reaction.

2.3. Preparation of liposomes

TAT modified liposomes (TAT-PEG-LP) and PEGylated liposomes (PEG-LP) were prepared by the thin film hydration methods as described previously (Qin et al., 2011). Briefly, various amounts of SPC/CHO/CHO-PEG$_{2000}$/CHO-PEG$_{2000}$-TAT (see Table 1) were dissolved in chloroform. Chloroform was then removed by rotary evaporation. The obtained thin film was kept in vacuum for over 6 h to completely remove the residual organic solvent. The thin film was hydrated in PBS (pH 7.4) for 1 h at 37 °C. Then it was further intermittently sonicated by a probe sonicator at 100 W for 50 s. And the TF modified liposomes (TF-PEG-LP) were prepared according to a post-insertion method (Yang et al., 2008) in which CHO-PEG$_{3500}$-TF micelles was prepared in advance using the above method and then incubated with the matrix liposomes (PEG-LP) for 1 h at 37 °C, As shown in Fig. 2, the dual-ligand liposomes (TAT/TF-PEG-LP) were prepared according to the aforesaid post-insertion method with the matrix liposomes PEG-LP replaced by TAT-PEG-LP.

2.4. Size and zeta potential measurements

The size and zeta potential of the liposomes were determined using a Malvern Zetasizer Nano ZS90 instrument (Malvern instruments Ltd., UK). Prior to measurement, 100 μl of the sample (lipid concentration 2.1 mg/ml) was diluted to 1 ml using the same buffer.

2.5. Cellular uptake in vitro

2.5.1. Cell culture

HepG2 cells, A2780 cells and HUVECs were grown in RPMI-1640 medium (GIBCO), DMEM medium (GIBCO) and DMEM medium (GIBCO), respectively, which contained 10% FBS, 100 μg/ml streptomycin, and 100 U/ml penicillin. The cells were maintained at 37 °C in a humidified incubator with 5% CO_2.

2.5.2. Evaluation of the expression of TF receptors

HepG2 cells, A2780 cells and HUVECs were washed with PBS (pH 7.4) and detached by treatment with trypsin, respectively. Detached cells were incubated with FITC labeled anti-CD71 antibodies for 30 min at 37 °C. Ten thousand cells per sample were analyzed using a BDFACSAria™ II flow cytometer (BD, San Jose, CA, USA).

2.5.3. Quantitative evaluation of cellular uptake by confocal laser scanning microscopy (CLSM)

Liposomes labeled with CFPE were prepared as described above, with the probe CFPE added to the lipid materials at first. HepG2 cells, A2780 cells and HUVECs were plated on gelatin-coated cover slips in 6-well culture plates and cultured for 48 h. Different formulations of liposomes were added to the plates with a total lipid concentration of 0.21 mg/ml. After incubation for 4 h at 37 °C under 5% CO_2, the cells were washed three times with cold PBS (pH 7.4) and 2 ml 2 μg/ml DAPI was added for 5 min, then cells were washed again and fixed using 4% paraformaldehyde. Cover slips were mounted cell-side down with slides and viewed using a Leica TCS SP5 AOBS confocal microscopy system (Leica, Germany).

2.5.4. Quantitative evaluation of cellular uptake by flow cytometer

Liposomes labeled with CFPE were prepared as described above. HepG2 cells, A2780 cells and HUVECs were plated on gelatin-coated cover slips in 6-well culture plates and cultured for 48 h. Different formulations of liposomes were added to the plates with a total lipid concentration of 0.21 mg/ml. After incubation at 37 °C under 5% CO_2 for 4 h, the cells were detached by treatment with trypsin for five minutes, washed three times with cold PBS and finally resuspended in 0.5 ml PBS for flow cytometry measurement.

2.6. Evaluation of delivery efficiency in vivo

2.6.1. Tumor-bearing mice models

Nude mice weighing 20–25 g were purchased from Experiment Animal Center of Sichuan University (PR China). All the animal experiments adhered to the principles of care and use of laboratory animals and were approved by the Experiment Animal Administrative Committee of Sichuan University.

Tumor-bearing mice were established as following method. Briefly, nude mice were inoculated subcutaneously with 1×10^6 HepG2 cells in the left flank. These models can be used for experiment when the diameter of tumor reached about 10 mm.

2.6.2. Ex vivo DiD dye fluorescence imaging

To evaluate the bio-distribution of liposomes in tumor bearing mice, DiD was used as a fluorescent probe for *ex vivo* fluorescence imaging (Ntziachristos et al., 2003; Zhang et al., 2010). And the

Table 1
Composition of liposomes (mol%) and their size and zeta potential.

Abbreviations	Corresponding compositions			Physical properties		
	SPC (%)	CHO (%)	Functional cholesterol lipids composition	Size (nm)	PDI	Zeta (mV)
TAT/TF-PEG-LP	65.0	29.0	4%CHO-PEG_{2000}/1% CHO-PEG_{2000}-TAT/1% CHO-PEG_{3500}-MAL	130.17 ± 8.32	0.191 ± 0.028	4.64 ± 0.42
TAT-PEG-LP	65.0	29.0	5%CHO-PEG_{2000}/1% CHO-PEG_{3500}-TAT	122.60 ± 3.66	0.209 ± 0.025	9.04 ± 0.92
TF-PEG-LP	65.0	29.0	5%CHO-PEG_{2000}/1% CHO-PEG_{2000}-MAL	127.10 ± 5.30	0.188 ± 0.022	0.547 ± 0.19
PEG-LP	65.0	29.0	6% CHO-PEG2000	112.00 ± 5.37	0.158 ± 0.009	−0.424 ± 0.37

The data represented the mean ± SD ($n = 3$).

DiD-loaded liposomes were prepared by the method described above, with DiD added to the lipid materials at first. The DiD-loaded TAT/TF-PEG-LP, TAT-PEG-LP, TF-PEG-LP and PEG-LP were injected into HepG2 tumor-bearing nude mice at a dose of 10 mg lipids/kg *via* the tail vein. 24 h later, the mice were executed by cervical dislocation. The whole tumors were removed and washed with cold PBS. Then the images were captured by the CCD camera (Quick View 3000, Bio-Real, Austria).

2.6.3. Qualitative analysis of delivery efficiency

To qualitatively investigate the delivery profiles of liposomes *in vivo*, The DiD-loaded TAT/TF-PEG-LP, TAT-PEG-LP, TF-PEG-LP and PEG-LP were injected into HepG2 tumor-bearing nude mice at a dose of 10 mg lipids/kg *via* the tail vein. 24 h later, the mice were executed by cervical dislocation, and tumors were excised and put in liquid nitrogen immediately. Then tumors were frozen sectioned (4 μm in thickness). Sections were stained with DAPI (2 μg/ml) for 5 min, washed three times with cold PBS, and then observed *via* CLSM.

2.6.4. Quantitative determination of delivery efficiency

The quantitative determination by flow cytometry was performed to further evaluate the delivery efficiency of liposomes into tumors. The manner was similar to the previously described methods with some modification (Kirpotin et al., 2006). After liposomes were injected into mice for 24 h, tumors were excised and cut into small pieces. Then the dissociation solution [Collagenase type IV (1 mg/ml) and DNase I (30 μg/ml)] was added at 37 °C for 1 h, following the process of sieving (70-μm mesh), centrifugation and washing with PBS for three times. Cells were finally resuspended in 0.5 ml PBS for flow cytometry measurement. And cells from tumor-bearing mice injected with PBS were served as blank.

2.7. Statistical analysis

Analysis of variance (ANOVA) was used to test the statistical significance of differences among groups. Statistical significance was evaluated by using Student's *t*-test or Dunnett's test for the single or multiple comparisons of experimental groups, respectively.

3. Results

3.1. Synthesis of CHO-PEG_{2000}-TAT

To prepare the TAT modified cholesterol derivate (CHO-PEG_{2000}-TAT), we first synthesized CHO-PEG_{2000}-MAL by conjugating the PEG with a maleimide group (-MAL) to the compound **5**, then linked TAT to the distal end of CHO-PEG_{2000}-MAL *via* a thioether bond. The structure of CHO-PEG_{2000}-MAL was verified by ^{1}H NMR (400 MHz,

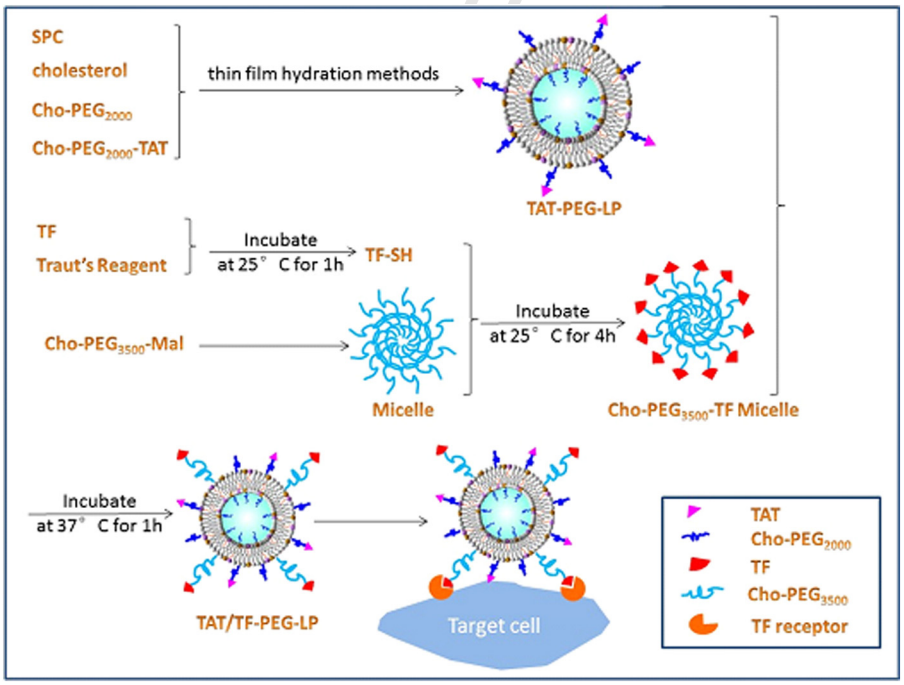

Fig. 2. Schematic illustration of the preparation method of dual-ligand liposomes.

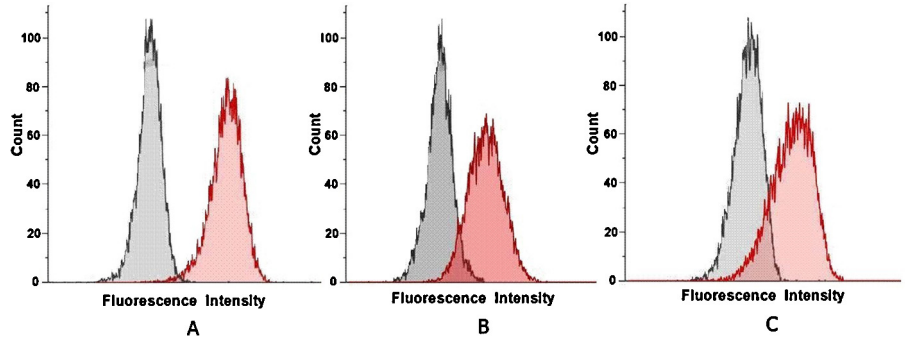

The fluorescence intensity of different cells

	A	B	C
Non-treated	3.25	2.62	6.47
Antibodies incubated	43.74	12.92	30.77

Fig. 3. Expression levels of TFR. The expression of TFR on HepG2 cells (A), A2780 cells (B) and HUVECs (C) was confirmed by flow cytometer as described in materials and methods. Black lines indicate non-treatment, and red lines indicate results obtained for the anti-CD71 antibody treatment. (For interpretation of the references to color in this figure legend, the reader is referred to the web version of this article.)

Q2

$CDCl_3$, δppm): 6.64 (s, 2H), 5.25 (s, 1H), 3.82–3.45 (br, m, PEG protons, ~181 H), 3.15–3.07 (m, 2H), 2.56 (s, 2H), 2.44 (t, 1H), 2.29–2.26 (m, 1H), 2.15–2.13 (m, 1H), 1.88–0.83 (m, CHO protons), with 0.675 (s, 3H), 0.89 (d, 6H), 0.91 (d, 3H,), 1.02 (s, 3H). TOF MS ES+ confirmed the formation of CHO-PEG_{2000}-TAT (M_w calculated = 4255 Da, M_w observed = 4356 Da). ^{1}H NMR was also used to confirm the structure of CHO-PEG_{2000}-TAT, whose PEG and TAT backbone could be found in ^{1}H NMR. In addition, the disappearance of double bond of MAL (6.64 (s, 2H)) also signified the form of thioether bond between CHO-PEG_{2000}-MAL and TAT (see supplementary material).

3.2. Characteristics of liposomes

Liposome size measurements showed that the sizes of all the liposomes were mainly about 120 nm; the zeta potential of TF-PEG-LP and PEG-LP was nearly neutral, while TAT-PEG-LP was obviously positive charged, and the positive charge of TAT/TF-PEG-LP was lower than that of TAT-PEG-LP (Table 1).

3.3. Detection of TF receptor expression

To evaluate the expression of the TF receptors on different cell surfaces, flow cytometric analyses of HepG2 cells, A2780 cells and HUVECs were carried out using FITC labeled anti-CD71 antibodies (Fig. 3). The ratios of fluorescence intensity (cells incubated with antibodies to non-treated cells) which reflected the expression level of TFR were 13.45 (HepG2 cells), 4.93 (A2780 cells) and 4.76 (HUVECs), respectively. It revealed that HepG2 cells expressed substantial TFR, while fewer on the surface of A2780 cells and HUVECs.

3.4. Qualitative evaluation of cellular uptake in vitro by confocal laser scanning microscopy (CLSM)

The cellular uptake of different liposomes (see Table 1) in HepG2 cells, A2780 cells and HUVECs were investigated by CLSM, as shown in Fig. 4a. The dual-ligand liposomes (TAT/TF-PEG-LP) resulted in stronger fluorescence signals inside the HepG2 cells than the single-ligand liposomes (TAT-PEG-LP or TF-PEG-LP), indicating that TAT/TF-PEG-LP was efficiently internalized by the HepG2 cells under the synergistic effect of both ligands. However, in HUVECs, whose TFR expression levels were lower, the difference of cellular uptake between TAT/TF-PEG-LP and TAT-PEG-LP was not as obvious as that in HepG2 cells (Fig. 4c). And in A2780 cells, the cellular uptake difference of TAT/TF-PEG-LP and TAT-PEG-LP was between HepG2 cells and HUVECs.

3.5. Quantitative evaluation of cellular uptake in vitro by flow cytometer

Then the cellular uptake of different liposomes (see Table 1) was quantitatively evaluated using flow cytometer. As shown in Fig. 5a, compared to the control liposome PEG-LP, the cellular uptake of TAT-PEG-LP, TF-PEG-LP and TAT/TF-PEG-LP was respectively increased by 2.33, 2.33 and 22.17 times in HepG2 cells. In this type of cell line, which expressed substantial TFR on surface, the cellular uptake amount of TAT/TF-PEG-LP was far more than that of TAT-PEG-LP plus TF-PEG-LP, so the synergistic effect of both ligands on cellular uptake was obvious. However in the case of HUVECs (Fig. 5c), whose TFR expression levels were lower, there was not synergetic effect of TAT/TF-PEG-LP on cellular uptake, the uptake amount of TAT-PEG-LP, TF-PEG-LP and TAT/TF-PEG-LP was 1.05, 9.42 and 8.32-fold higher than that of control liposome PEG-LP. And in A2780 cells (Fig. 5b), the synergetic effect of TAT/TF-PEG-LP on cellular uptake was between HepG2 cells and HUVECs. The uptake amount of TAT-PEG-LP, TF-PEG-LP and TAT/TF-PEG-LP was 4.88, 1.48 and 11.85-fold higher than that of control liposome PEG-LP.

3.6. Ex vivo DiD dye fluorescence imaging

Ex vivo NIR fluorescence imaging was performed on excised mice tumors. As shown in Fig. 6, a strong NIR fluorescent signal from the tumors of the mice injected intravenously with the DiD-loaded TAT/TF-PEG-LP and TF-PEG-LP were observed 24 h after injection. Tumors from mice treated with TAT-PEG-LP and PEG-LP had weaker signal compared to TAT/TF-PEG-LP and TF-PEG-LP. Control animal injected with saline solution produced no background signal.

3.7. Qualitative analysis of delivery efficiency in vivo

The tumor sections from HepG2 tumor-bearing mice that received DiD loaded PEG-LP, TAT-PEG-LP, TF-PEG-LP and TAT/TF-PEG-LP were qualitatively analyzed using confocal laser scanning microscopy. As illustrated in Fig. 7, the tumor frozen section of TAT/TF-PEG-LP group showed strongest red fluorescence (fluorescence of DiD). TAT-PEG-LP group showed some red fluorescence but weaker than TAT/TF-PEG-LP group. TF-PEG-LP and PEG-LP groups showed little red fluorescence and had no obvious difference. The

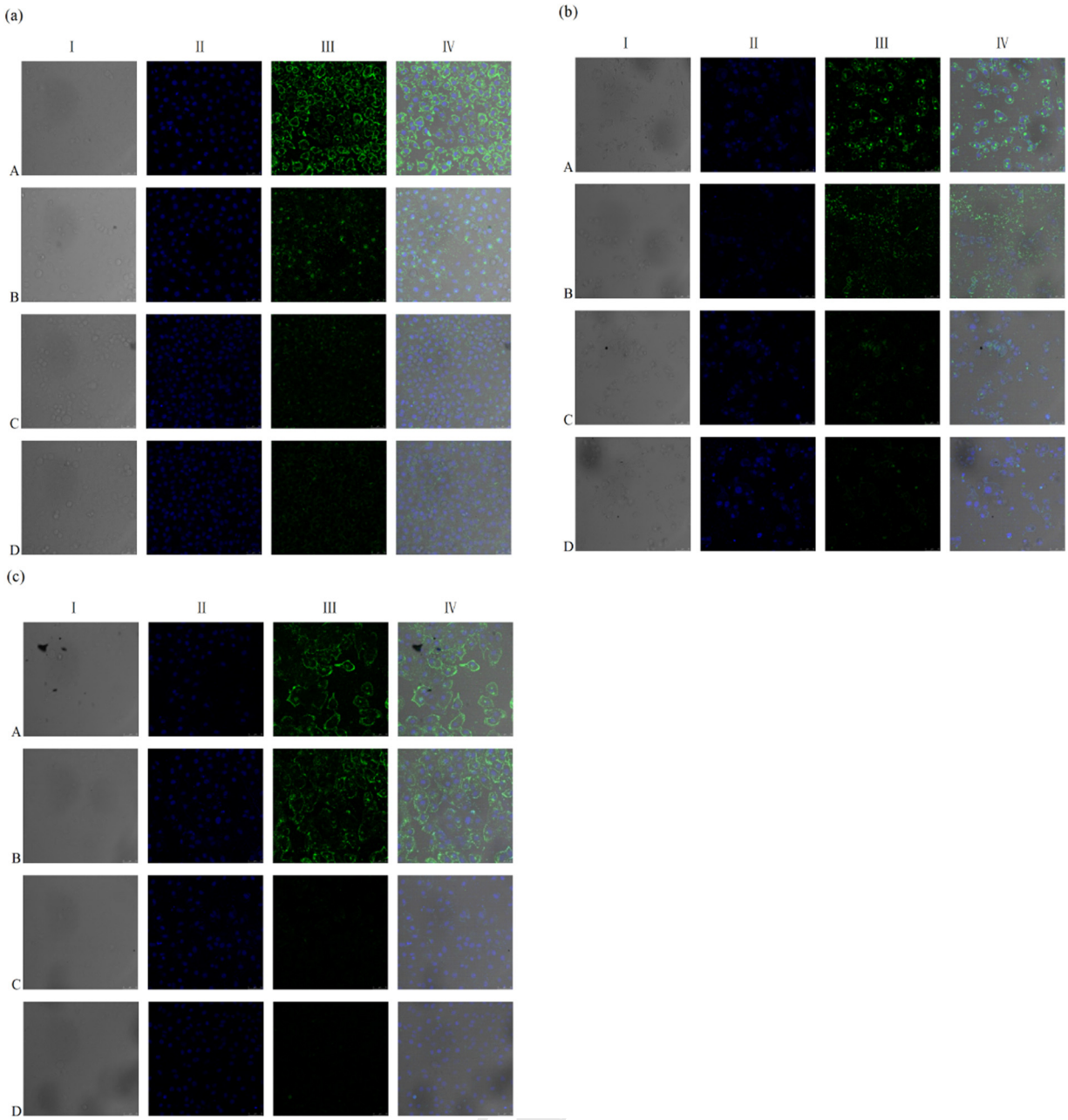

Fig. 4. CLSM images of HepG2 cells (a), A2780 cells (b) and HUVECs (c) incubated with different formulations of CFPE-labeled liposomes at 37 °C for 4 h. A, TAT/TF-PEG-LP; B, TAT-PEG-LP; C, TF-PEG-LP; D, PEG-LP. The row I was the bright field. The blue fluorescence exhibited in row II was due to DAPI-staining of the nuclei. The green fluorescence exhibited in row III was due to the CFPE-labeled liposomes. The forth row was the overlay sight. (For interpretation of the references to color in this figure legend, the reader is referred to the web version of this article.)

result indicated that efficient targeted delivery of DiD was achieved by the dual-ligand modified liposomes.

3.8. Quantitative determination of delivery efficiency in vivo

The cytometric data allowed for quantitative analysis of the results was obtained from treated HepG2 tumor-bearing mice (Fig. 8). The fluorescent intensity represented cellular uptake amount of different liposomes in tumor tissues. The fluorescent intensity of the group receiving TAT/TF-PEG-LP was 1.31, 1.37 and 1.45-fold higher than that of the groups receiving TAT-PEG-LP, TF-PEG-LP and PEG-LP, respectively. The result further demonstrated that an efficient targeted delivery of DiD could be achieved by the dual-ligand modified liposomes *in vivo*.

4. Discussion

The ability of carriers to specifically targeting delivery cargoes to tumors is important to effective cancer therapy. The active tumor targeted liposomes, which were modified with some specific ligands such as transferrin, folic acid, peptides or antibodies, could selectively recognize and bind to the specific receptor over-expressed on tumor cells, then result in increased targeting efficiency and less toxicity. However, the presence of receptor-targeting moiety alone on PEGylated liposomes limits the cellular uptake of liposomes due to receptor saturation (Sharma et al., 2012); Harashima et al. also indicated that some kind of the ligand modified carriers enter cells *via* the receptor mediated endocytosis which is a saturated pathway, the saturation phenomenon might

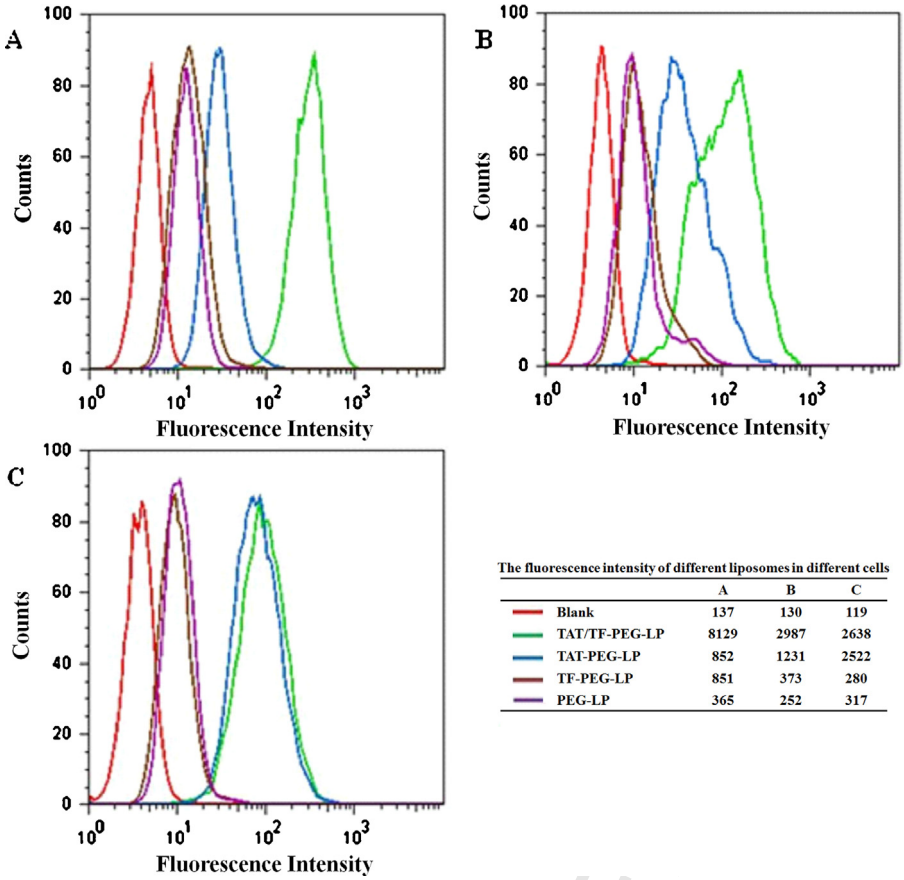

The fluorescence intensity of different liposomes in different cells

	A	B	C
Blank	137	130	119
TAT/TF-PEG-LP	8129	2987	2638
TAT-PEG-LP	852	1231	2522
TF-PEG-LP	851	373	280
PEG-LP	365	252	317

Fig. 5. Fluorescence intensity of HepG2 cells (a), A2780 cells (b) and HUVECs (c) measured by flow cytometer after incubated with different formulations of CFPE labeled liposomes at 37 °C for 4 h. Blank (red lines), TAT/TF-PEG-LP (green lines), TAT-PEG-LP (blue lines), TF-PEG-LP (brown lines) and PEG-LP (purple lines). (For interpretation of the references to color in this figure legend, the reader is referred to the web version of this article.)

limit the cellular uptake of ligand modified liposomes (Kibria et al., 2011). To generate further therapeutic efficacy, TAT which could promote carriers to enter cells effectively *via* an unsaturated and receptor/transporter independent pathway (Torchilin et al., 2001) was applied to develop the dual-ligand liposomes (Fig. 2). In this liposomal formulation, the receptor targeting property of transferrin was combined with the enhanced cell uptake effect of TAT to improve the transport of desired cargoes to tumor. In previous studies, phospholipids have been extensively employed as an anchor for both PEGylation and ligand modifying in liposomal formulations. However, DSPE introduced a negative charge to the liposomes surface, which might lead to additional plasma protein binding (Zhao et al., 2007). In contrast, cholesterol was electrically neutral. Besides, cholesterol is more chemically stable and much cheaper than DSPE. Thus, we presumed cholesterol anchor may have many advantages over DSPE anchor. Furthermore, to ensure that the functional cholesterol derivative lipids were stable during circulation, we chose the ether linkage to connect the cholesterol anchor with PEG or ligands instead of the commonly used ester bond which could be hydrolyzed by the esterase in the plasma (Xu et al., 2008; Heyes et al., 2006). In this study, we aimed to develop a dual-ligand drug delivery system (TAT/TF-PEG-LP) to enhance the targeting selectivity and cellular uptake efficiency both *in vitro* and *in vivo*, in which TAT and TF were steadily connected with the cholesterol anchor *via* a stable ether linkage. The size data (Table 1) and the transmission electron micrographs (see supplementary material) showed that the dual-ligand liposomes kept the perfect liposome structure and dispersed uniformly.

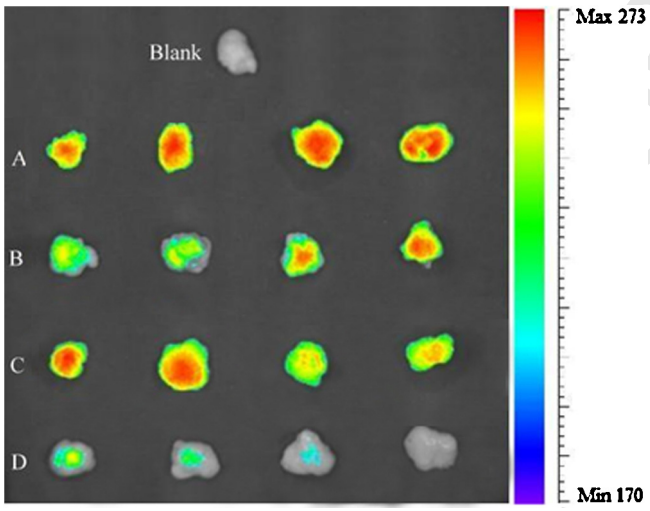

Fig. 6. *Ex vivo* imaging of tumors given different liposomes *via* tail vein. A, TAT/TF-PEG-LP; B, TAT-PEG-LP; C, TF-PEG-LP; D, PEG-LP; Blank, saline ($n = 4$).

In previous studies, cationic macromolecules have been reported to trigger thrombosis, embolization and hemolysis *in vivo* (Antohi and Brumfeld, 1984; Zhu et al., 2007). Therefore, the presence of cationic peptides such as TAT on the liposomal surface can induce some undesirable side effect. The presence of cationic peptides TAT on liposomes can induce interactions with the erythrocyte membrane causing cell lysis and release of hemoglobin (see supplementary material). Furthermore, the TAT was known as a nonspecific molecule, which penetrates any cells. And in this study, we utilized the PEG chain length difference of two functional

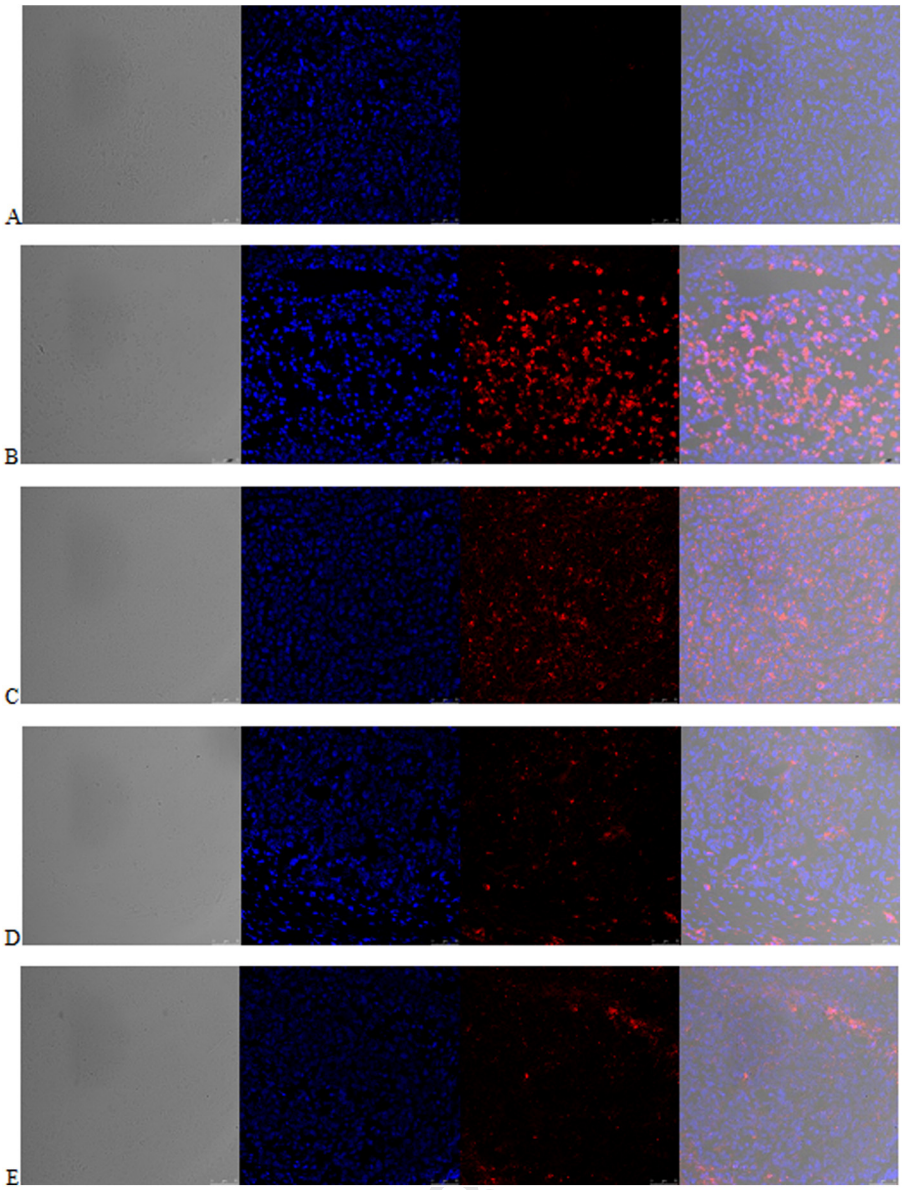

Fig. 7. CLSM images of HepG2 tumor frozen sections from tumor-bearing mice receiving different formulations of DiD loaded liposomes. A, blank; B, TAT/TF-PEG-LP; C, TAT-PEG-LP; D, TF-PEG-LP; E, PEG-LP. The row I was the bright field. The blue fluorescence exhibited in row II was due to DAPI-staining of the nuclei. The red fluorescence exhibited in row III was due to the DiD loaded liposomes. The forth row was the overlay sight. (For interpretation of the references to color in this figure legend, the reader is referred to the web version of this article.)

materials (CHO-PEG-TF and CHO-PEG-TAT) in the dual-ligand liposomal formulations to ensure that TAT could be shielded during circulation. To make sure the dual-ligand liposomes possess the strongest synergistic effect on cellular uptake and proper masking effect to the non-specific TAT, the PEG chain length of ligand which could affect the cell binding and cellular uptake should be first identified (see supplementary material). The result showed that the PEG chain length combinations of CHO-PEG_{2000}-TAT/CHO-PEG_{3500}-TF could make the dual-ligand liposomes achieve the most effective synergistic effect on cellular uptake, and in this condition, as shown in Table 1, the positive charge of TAT/TF-PEG-LP was lower than that of TAT-PEG-LP, which indicated that the TAT could be masked by the longer PEG chain of CHO-PEG_{3500}-TF to some extent. Then the hemolytic toxicity of TAT/TF-PEG-LP was much lower than that of TAT-PEG-LP in the hemolysis assay (see supplementary material). So that we speculated the non-specificity, toxicity and instability of liposomes caused by TAT could be overcame *in vivo*, which need to be further proved in the future research.

In this study, we evaluated the synergetic effect of both ligands and verified the targeting specificity of dual-ligand liposomes *via* cellular uptake by three kinds of cells which possessed different expression levels of TFR on their surface (Fig. 3). As shown in Fig. 5, compared to the control liposome PEG-LP (purple lines), although the single-ligand liposomes TAT-PEG-LP (blue lines) increased the cellular uptake amount to some degree, it exhibited no regularity in three different cells lines due to the non-specificity of TAT, while the other single-ligand liposomes TF-PEG-LP (brown lines) only showed a slight enhancement on cellular uptake in HepG2 cells and A2780 cells due to receptor saturation. However, the dual-ligand liposomes TAT/TF-PEG-LP exhibited the enhanced cellular uptake and selectivity at the same time. As shown in Fig. 5a, the cellular uptake amount of TAT/TF-PEG-LP was far more than that of PEG-LP, TAT-PEG-LP and TF-PEG-LP in HepG2 cells which expressed substantial TFR on surface, and the synergistic effect of TAT/TF-PEG-LP on cellular uptake varied from the cells to cells, when the expression level of TFR on cell surface was lower (such as HUVECs),

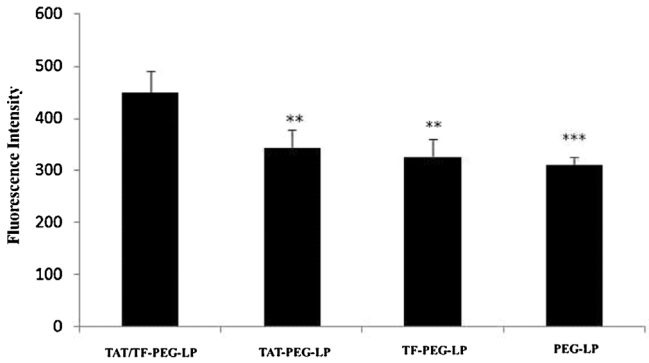

Fig. 8. Cytometric quantitation of cell suspensions from HepG2 tumor-bearing nude mice receiving different formulations of DiD loaded liposomes. Data represented the mean ± SD. $^{*}P < 0.05$; $^{**}P < 0.01$, $^{***}P < 0.001$, *versus* TAT/TF-PEG-LP.

TAT/TF-PEG-LP could not recognize and bind with target cell by the TF motif efficiently, hence the cellular uptake of TAT/TF-PEG-LP was mainly mediated by TAT and almost the same as that of TAT-PEG-LP (Fig. 5c). The result indicated that only when the amount of TFR on cells reached a certain point would the synergetic effect between TAT and TF motif start to appear. It is reported that many tumor cells expressed much more TFR than normal cells, so the dual-ligand liposomes in our study were expected to achieve the effective synergistic targeted delivery. In this condition, the dual-ligand liposomes attached to TFR on the tumor cell surface *via* the specific ligand TF, then penetrated into tumor cells with high efficiency predominantly mediated by TAT (Fig. 2). Consistently, the CLSM analysis also confirmed the significant synergetic effect of dual-ligand liposomes on cellular uptake in HepG2 cells (Fig. 4a) and it was more obvious than in A2780 cells and HUVECs (Fig. 4b and c), strengthening the point of view that the dual-ligand liposomes possessed increased cellular uptake efficiency and target specificity *in vitro*.

The *in vivo* experiments were performed on the HepG2 tumor-bearing nude mice, which had higher TFR expressed on the cell surface in tumor tissue. Fig. 6 exhibited that the tumor distributions of TAT/TF-PEG-LP and TF-PEG-LP were higher than that of PEG-LP owing to the active targeting effect of TF motif. We could also see that the signal from tumors of the mice treated with TAT-PEG-LP was fairly weak due to the non-specificity and instability of liposomes caused by TAT. However, the *ex vivo* imaging of tumors only reflected the accumulation capacity of liposomes in tumor tissues but not the ability to enter cells. Then there was not clear signal difference between TF-PEG-LP and TAT/TF-PEG-LP in Fig. 6 because the targeting ability of liposomes largely depends upon the passive targeting of PEGylation and the active targeting of TF motif. Although TAT/TF-PEG-LP and TF-PEG-LP had the similar distributions in tumors, after they arrive at tumor tissues, with the help of TAT, the ability for delivery of payload into cells of TAT/TF-PEG-LP was much stronger than that of TF-PEG-LP according to the qualitative (Fig. 7) and quantitative evaluations (Fig. 8). As shown in Fig. 7 the tumor frozen sections of TF-PEG-LP and PEG-LP groups had little red fluorescence (fluorescence of DiD), indicating that although TF modified liposome could achieve the active targeting *in vivo* according to the previous studies (Hong et al., 2010), it could not more efficiently target DiD into tumor cells *in vivo* due to receptor saturation. This point was further certified by the cytometric data *in vivo* (Fig. 8). And the cellular uptake amount of TAT/TF-PEG-LP in tumor tissues was higher than that of the three other liposomes (Figs. 7 and 8). The results might be induced by the increased targeting specificity mediated by TF motif and the enhanced cellular uptake efficiency predominantly mediated by TAT. Besides, the aqueous layer of CHO-PEG$_{3500}$-TF of liposomes could partially mask the positive charge of TAT, thus increasing the stability of liposomes *in vivo*. These results demonstrated that an efficient targeted delivery of payload could be achieved by the dual-ligand modified liposomes *in vivo*.

5. Conclusions

In this study, we successfully developed the dual-ligand liposomes modified with the specific ligand TF motif and non-specific TAT. This liposomal delivery system possessed increased cellular uptake efficiency and targeting specificity in the cells whose TFR expression levels were high, and achieved an efficient synergistic targeted delivery of payload into tumor cells in HepG2 tumor-bearing nude mice.

Acknowledgments

The work was funded by the National Natural Science Foundation of China (81072599), the National Basic Research Program of China (973 Program, 2013CB932504) and the School of Pharmacy, Fudan University & the Open Project Program of Key Lab of Smart Drug Delivery, Ministry of Education & PLA, China. The authors thank Professor Zhenlei Song for providing help on the synthesis of cholesterol derivative lipids.

Appendix A. Supplementary data

Supplementary data associated with this article can be found, in the online version, at http://dx.doi.org/10.1016/j.ijpharm.2013.06.048.

References

Anabousi, S., Bakowsky, U., Schneider, M., Huwer, H., Lehr, C.M., Ehrhardt, C., 2006. In vitro assessment of transferrin-conjugated liposomes as drug delivery systems for inhalation therapy of lung cancer. Eur. J. Pharm. Sci. 29, 367–374.
Antohi, S., Brumfeld, V., 1984. Polycation-cell surface interactions and plasma membrane compartments in mammals. Interference of oligocation with polycationic condensation. Z. Naturforsch. C 39, 767–775.
Banks, W.A., Robinson, S.M., Nath, A., 2005. Permeability of the blood-brain barrier to HIV-1 TAT. Exp. Neurol. 193, 218–227.
Brooks, H., Lebleu, B., Vive's, E., 2005. Tat peptide-mediated cellular delivery: back to basics. Adv. Drug Deliv. Rev. 57, 559–577.
Chiu, S-J., Liu, S., Perrotti, D., Marcucci, G., Lee, R.J., 2006. Efficient delivery of a Bcl-2-specific antisense oligodeoxyribonucleotide (G3139) via transferrin receptor-targeted liposomes. J. Control Release 112, 199–207.
Gabizon, A., Horowitz, A.T., Goren, D., Tzemach, D., Shmeeda, H., Zalipsky, S., 2003. In vivo fate of folate-targeted polyethylene-glycol liposomes in tumor-bearing mice. Clin. Cancer Res. 9, 6551–6559.
Gupta, B., Levchenko, T.S., Torchilin, V.P., 2005. Intracellular delivery of large molecules and small particles by cell-penetrating proteins and peptides. Adv. Drug Deliv. Rev. 57, 637–651.
Hatakeyama, H., Akita, H., Maruyama, K., Suhara, T., Harashima, H., 2004. Factors governing the in vivo tissue uptake of transferrin-coupled polyethylene glycol liposomes in vivo. Int. J. Pharm. 281, 25–33.
Heyes, J., Hall, K., Tailor, V., Lenz, R., MacLachlan, I., 2006. Synthesis and characterization of novel poly(ethylene glycol)–lipid conjugates suitable for use in drug delivery. J. Control Release 112, 280–290.
Hong, M., Zhu, S., Jiang, Y., Tang, G., Sun, C., Fang, C., Shi, B., Pei, Y., 2010. Novel anti-tumor strategy: PEG–hydroxycamptothecin conjugate loaded transferrin–PEG-nanoparticles. J. Control Release 141, 22–29.
Kibria, G., Hatakeyama, H., Ohga, N., Hida, K., Harashima, H., 2011. Dual-ligand modification of PEGylated liposomes shows better cell selectivity and efficient gene delivery. J. Control Release 153, 141–148.
Kirpotin, D.B., Drummond, D.C., Shao, Y., Shalaby, M.R., Hong, K., Nielsen, U.B., Marks, J.D., Benz, C.C., Park, J.W., 2006. Antibody targeting of long-circulating lipidic nanoparticles does not increase tumor localization but does increase internalization in animal models. J. Cancer Res. 66, 6732–6740.
McNeeley, K.M., Annapragada, A., Bellamkonda, R.V., 2007. Decreased circulation time offsets increased efficacy of PEGylated nanocarriers targeting folate receptors of glioma. Nanotechnology 18, 385101 (11 pp).
Ntziachristos, V., Bremer, C., Weissleder, R., 2003. Fluorescence imaging with near-infrared light: new technological advances that enable in vivo molecular imaging. Eur. Radiol. 13, 195–208.

Pan, X., Wu, G., Yang, W., Barth, R.F., Tjarks, W., Lee, R.J., 2007. Synthesis of cetuximab-immunoliposomes via a cholesterol-based membrane anchor for targeting of EGFR. Bioconj. Chem. 18, 101–108.
Qin, Y., Chen, H., Yuan, W., Kuai, R., Zhang, Q., Xie, F., Zhang, L., Zhang, Z., Liu, J., He, Q., 2011. Liposome formulated with TAT-modified cholesterol for enhancing the brain delivery. Int. J. Pharm. 419, 85–95.
Sharma, G., Modgil, A., Sun, C., Singh, J., 2012. Grafting of cell-penetrating peptide to receptor-targeted liposomes improves their transfection efficiency and transport across blood-brain barrier model. J. Pharm. Sci. 101, 2468–2478.
Shohda, K.-i., Sugawara, T., 2006. DNA polymerization on the inner surface of a giant liposome for synthesizing an artificial cell model. R. Soc. Chem. 2, 402–408.
Singh, M., 1999. Transferrin as a targeting ligand for liposomes and anticancer drugs. Curr. Pharm. Des. 5, 443–451.
Suzuki, R., Takizawa, T., Kuwata, Y., Mutoh, M., Ishiguro, N., Utoguchi, N., Shinohara, A., Eriguchi, M., Yanagie, H., Maruyama, K., 2007. Effective anti-tumor activity of oxaliplatin encapsulated in transferrin–PEG-liposome. Pharm. Nanotechnol. 346, 143–150.
Torchilin, V.P., Rammohan, R., Weissig, V., Levchenko, T.S., 2001. TAT peptide on the surface of liposomes affords their efficient intracellular delivery even at low temperature and in the presence of metabolic inhibitors. Proc. Nat. Acad. Sci. 98, 8786–8791.
Wadia, J.S., Dowdy, S.F., 2002. Protein transduction technology. Curr. Opin. Biotechnol. 13, 52–56.
Xu, H., Deng, Y., Chen, D., Hong, W., Lu, Y., Dong, X., 2008. Esterase-catalyzed dePEGylation of pH-sensitive vesicles modified with cleavable PEG-lipid derivatives. J. Control Release 130, 238–245.
Yang, X., Koh, C.G., Liu, S., Pan, X., Santhanam, R., Yu, B., Peng, Y., Pang, J., Golan, S., Talmon, Y., Jin, Y., Muthusamy, N., Byrd, J.C., Chan, K.K., Lee, L.J., Marcucci, G., Lee, R.J., 2008. Transferrin receptor-targeted lipid nanoparticles for delivery of an antisense oligodeoxyribonucleotide against Bcl-2. Mol. Pharm. 6, 221–230.
Zhang, C., Liu, T., Su, Y., Luo, S., Zhu, Y., Tana, X., Fan, S., Zhang, L.L., Zhou, Y., Cheng, T.M., Shi, C.M., 2010. A near-infrared fluorescent heptamethine indocyanine dye with preferential tumor accumulation for in vivo imaging. Biomaterials 31, 6612–6617.
Zhao, X., Muthusamy, N., Byrd, J.C., Lee, R.J., 2007. Cholesterol as a bilayer anchor for PEGylation and targeting ligand in folate-receptor-targeted liposomes. J. Pharm. Sci. 96, 2424–2435.
Zhu, S., Qian, F., Zhang, Y., Tang, C., Yin, C., 2007. Synthesis and characterization of PEG modified N-trimethyl amino ethyl methacrylate chitosan nanoparticles. Eur. Polym. J. 43, 2244–2253.

Please cite this article in press as: Tang, J., et al., Synergistic targeted delivery of payload into tumor cells by dual-ligand liposomes co-modified with cholesterol anchored transferrin and TAT. Int J Pharmaceut (2013), http://dx.doi.org/10.1016/j.ijpharm.2013.06.048